Dynamic Model of a Supercritical Fluid Extraction Plant

João Fernandes
REQUIMTE, Departamento de Química, Faculdade de Ciências e Tecnologia, Universidade Nova de Lisboa, 2829-516 Caparica, Portugal

Rui Ruivo
Instituto de Tecnologia Química e Biológica (ITQB/UNL), Av. da República (EAN), 2781-901 Oeiras, Portugal

Pedro Simões
REQUIMTE, Departamento de Química, Faculdade de Ciências e Tecnologia, Universidade Nova de Lisboa, 2829-516 Caparica, Portugal

DOI 10.1002/aic.11123
Published online February 14, 2007 in Wiley InterScience (www.interscience.wiley.com).

A dynamic model of a supercritical fluid extraction (SFE) process was developed and applied to the fractionation of the binary mixture squalene/methyl oleate by supercritical carbon dioxide. The model combines a mathematical model for each main piece of equipment of the SFE process, namely, the countercurrent packed extraction column, the separation column for oil recovery and solvent regeneration, the heat exchanger for heating fresh CO_2, and the make-up of solvent in the process plant. Experimental tests were performed in a pilot-plant SFE apparatus where perturbations on prespecified operating parameters were induced and their effect on main process variables determined. A good agreement was obtained between experimental and predicted results. In addition, the dynamic model of the packed extraction column was applied to other SFE case studies where sufficient experimental data is available. The dynamic model was found to correctly predict the outlet streams composition profiles of all the case studies. © 2007 American Institute of Chemical Engineers *AIChE J,* 53: 825–837, 2007

Keywords: supercritical fluid extraction, fractionation, dynamic model, carbon dioxide, mass transfer

Introduction

Supercritical fluid extraction (SFE) is a process that uses fluids at supercritical conditions to selectively extract substances from solid or liquid mixtures. High product quality can be accomplished by fine-tuning pressure and temperature conditions of the fluid.

Correspondence concerning this article should be addressed to P. Simões at pcs@dq.fct.unl.pt.

The design and optimization analysis of SFE processes require reliable computational tools to predict the multiphase flow dynamics as well as the dynamic process behavior of the overall SFE unit. These models should incorporate both the hydrodynamics of transport through the contacting device and interphase mass transfer, as well as the dynamics of the process. While the former are important in process design and dimensioning, the later are of fundamental importance for process control and optimization. Some work has been done on these subjects.[1–3] Cygnarowicz and Seider[1] developed a dynamic simulator of the β-carotene process recovery

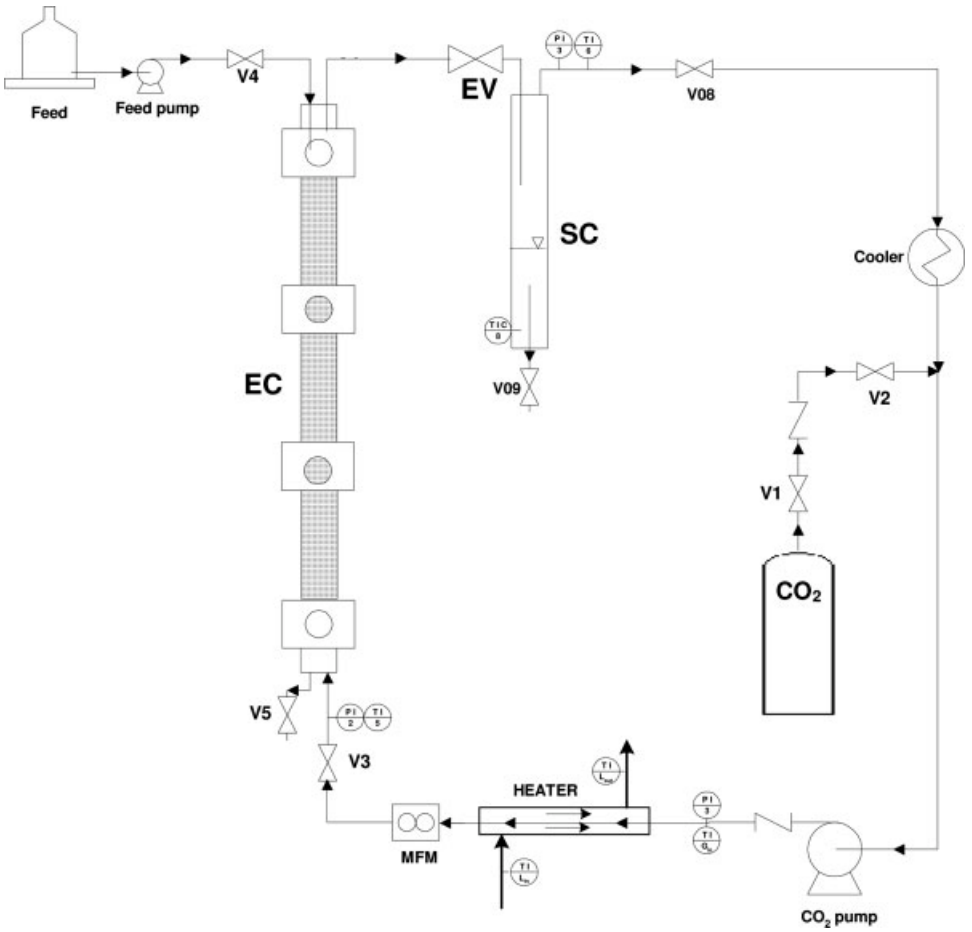

Figure 1. SFE plant.

from fermentation broths by SC CO_2, and analyzed the influence of induced disturbances on the feed and vapor flow rates on product separator pressure. A dynamic simulation model of the ethanol dehydration by SC propane was devised by Hytoft and Gani,[2] where the packed column was modeled as a multistage column. On the other hand, Ramchandran et al.[3] modeled a SFE plant for propanol/water extraction with the extraction column simulated as a tray-to-tray column. The influence of induced solvent flow disturbances in the process efficiency was analyzed.

Recently, we have presented an isothermal dynamic model of a SFE packed column, where mass transfer kinetics was addressed.[4] The extraction column, filled with structured gauze packing, was modeled by a multicomponent rate-based model where specific correlations for mass transfer and hydrodynamics[5] were introduced. As a case study, the simulation model was applied to the fractionation of a binary mixture made of squalene and methyl oleate by SC carbon dioxide. The thermodynamic equilibrium data of this system was modeled with the help of an empirical correlation for the oil loading in the gas phase (expressed as grams of solubilized oil per kilograms of carbon dioxide) and the separation factor between squalene and methyl oleate. A reasonable good agreement was obtained between the experimental and simulated results at several operating conditions of extraction.

The ultimate goal of this project was to develop a dynamic model of a whole SFE plant. In this way, the previous dynamic model of the extraction packed column was incorporated in a larger model where the heat exchanger for heating up the fresh supercritical solvent stream to the extraction column, the separation column for the recovery of extracted oil and regeneration of supercritical solvent, and the solvent make-up to the process were also integrated. The whole model of the SFE plant was then applied to the fractionation of the binary mixture squalene/methyl oleate by SC carbon dioxide. A comparison between the predicted data by the dynamic model and the experimental data obtained with a pilot-scale SFE apparatus is presented in this paper together with a critical analysis of the performance of the whole extraction process when subjected to load disturbances in prespecified process variables.

Finally, we tested the current dynamic model of the extraction packed column to other SFE processes. The purpose was to assess the general application of the model to SFE processes. The case studies were selected where sufficient experimental data was available in the literature and potential commercial application exists. The case studies under analysis in this work are the deacidification of virgin olive oil (VOO) by SC carbon dioxide,[6] the fractionation of olive oil deodorizer distillates (OODD),[7] and of shark liver oil (SLO)[8] by SC carbon dioxide. To test the effectiveness of

the dynamic model to other near-critical solvents besides carbon dioxide, we also applied the model to the fractionation of SLO by R134a.[9]

The SFE Process

Figure 1 shows a simplified flow diagram of a general SFE process. It partially resembles the pilot-scale SFE plant built in our laboratories and described elsewhere.[10] The main piece of a SFE plant for liquid mixtures is the extraction column, here labeled as EC. Typically, this is a stainless steel column filled with packing and operating at given extraction conditions of pressure and temperature. The oil feed, being denser than the supercritical solvent flows down EC, counter currently to carbon dioxide that rises up. Fresh solvent is introduced at the bottom of EC after being heated up to the required extracted temperature by a heat exchanger, labeled as HE. The simplest way to accomplish this is to use a double pipe type of heat exchanger; the required heat is supplied by a flux of hot liquid water flowing in a countercurrent way to the carbon dioxide flow in HE.

Contact between the two fluid phases is achieved throughout the whole packed bed in EC; the fluid phase, rich in carbon dioxide (the extract stream), leaves the column at the top. This phase contains the solutes that were dissolved by the solvent. The liquid phase, rich on oil (the raffinate stream), leaves the column at the bottom. A manual controlled valve, V5, depressurizes this stream and the oil is collected in a flask. The total amount of carbon dioxide dissolved in the raffinate stream is simply flashed to atmosphere after being measured with the help of a gas flow meter. The extract stream leaving the top of EC is depressurized by means of an electrically controlled valve, EV. It enters a second stainless steel column, labeled as separation column, SC, where the previously dissolved substances are separated from the solvent and collected by gravity at the bottom of the column; the regenerated carbon dioxide leaves SC by the top and is recirculated back to the extraction column after make-up to compensate for solvent losses in the extraction and separation columns.

The simulation of such SFE plant is important to fully understand the close relation between the several units of the plant and the associated operating parameter interactions to imposed disturbances on the SFE process. To simplify the current study, we opted to consider as a first approach the main units of the SFE process; it is foreseen that further units will be added to the current model in the future. The units included in the present model are the extraction column, the separation column, the heat exchanger to heat up fresh solvent stream to EC, and the make-up of solvent after the regeneration step. The simulation model of each one of the above pieces is described more detail in the next section.

Extraction column

Figure 2 presents a schematic representation of the counter current packed column. The dynamic simulation model of the extraction column is a multicomponent rate-based model. Since carbon dioxide has a nonnegligible solubility in the oil feed, the mass transfer rates of all components involved in the process are taken into account by the dynamic model.

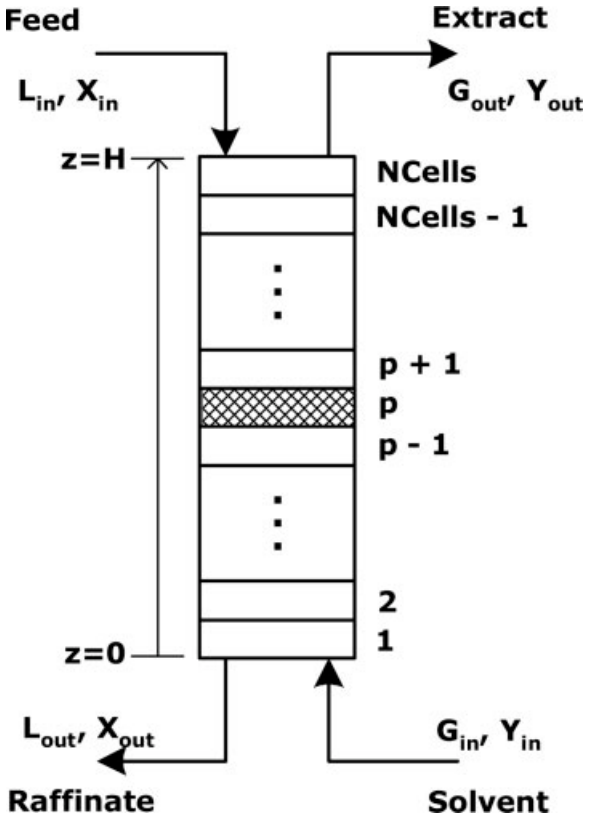

Figure 2. Extraction column.

The model comprises a set of partial differential equations corresponding to the differential material balances on the packed column and algebraic equations describing the mass transfer, the biphasic flow hydrodynamics in the packing, and the vapor–liquid equilibrium of the given system. The physical properties of the fluid phases are taken into account by incorporating correlations for each property as a function of the main operating variables. The differential material balances for component i in the gas and liquid phases are, respectively,

$$A\varepsilon\frac{\partial[(1-h_L)\rho_G Y_i]}{\partial t} = J_i - \frac{\partial(GY_i)}{\partial Z} \qquad \text{for} \quad i = 1\text{–}3 \quad (1)$$

$$A\varepsilon\frac{\partial[h_L\rho_L X_i]}{\partial t} = -J_i - \frac{\partial(LX_i)}{\partial Z} \qquad \text{for} \quad i = 1\text{–}3 \quad (2)$$

where h_L is the local liquid holdup and J_i the mass transfer fluxes of solute i. For methyl oleate and squalene J_i is positive if transfer occurs from the liquid to the gas phase; for carbon dioxide, J_i is positive in the reverse direction. Equations 1 and 2 are subjected to the following boundary conditions:

$$\begin{aligned} G &= G_{in},\ Y_i = Y_{i,in} \qquad \text{for } z = 0 \\ L &= L_{in},\ X_i = X_{i,in} \qquad \text{for } z = H \end{aligned} \quad (3)$$

The mass transfer fluxes are expressed in terms of overall mass transfer coefficients by applying the two-film theory of

multiphase mass transfer; thermodynamic equilibrium is assumed to occur at the interface of the two phases. Correlations for the mass transfer as well as the hydrodynamic phenomena were formerly developed for the ternary system squalene + methyl oleate + carbon dioxide.[4,5]

Separation column

Separation of the supercritical solvent from the previously extracted substances is achieved by depressurization in valve EV (Figure 1) and subsequent separation in SC, which basically works as a gravity-settler. A schematic representation of this column is shown in Figure 3. For simplification, it is assumed that pressure drop occurs prior to the entrance to SC and that cooling effects on EV valve body are neglected (in practice, this is experimentally achieved by installing a heating tape around the valve body; the heating tape controls the temperature of the expansion valve so that at the entrance of the separation column the temperature of the inlet gas phase can be kept reasonably constant and close to the desired value). Thermodynamic equilibrium is assumed to occur inside the separation column between the gas phase and the precipitated liquid phase. At a given time, gas and liquid holdups are at equilibrium, the exit streams, G^{OUT} and L^{OUT} are considered to be representative of the internal phases. The liquid holdup can be withdrawn continuously or a level control can be applied to the separation column. Depending on the case, the model is easily adapted to the condition chosen.

The separation column is modeled with a set of individual material balances plus the energy balance. If the liquid phase is continuously removed from the separation column, the set of equations is given by

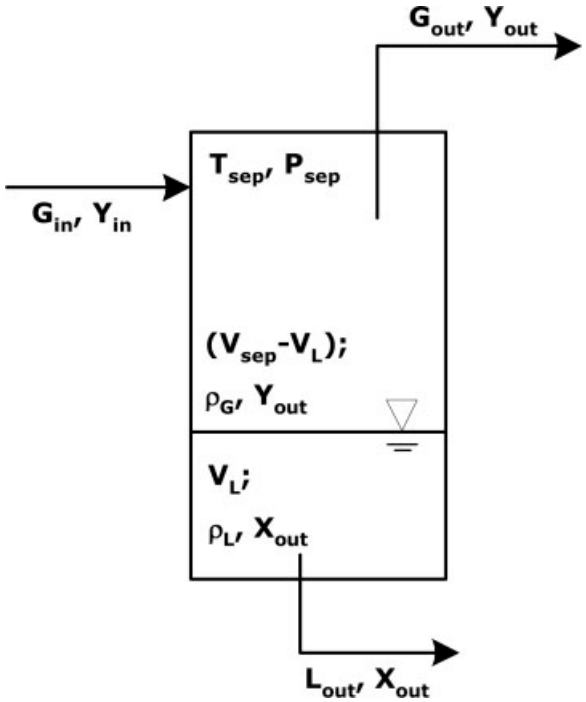

Figure 3. Regeneration column.

$$\frac{\partial[\rho_{\mathrm{L}} X_{\mathrm{OUT}_i} V_{\mathrm{L}}]}{\partial t} + \frac{\partial[\rho_{\mathrm{G}} Y_{\mathrm{OUT}_i}(V_{\mathrm{SEP}} - V_{\mathrm{L}})]}{\partial t} = G^{\mathrm{IN}} Y_i^{\mathrm{IN}} - G^{\mathrm{OUT}} Y_i^{\mathrm{OUT}} - L^{\mathrm{OUT}} X_i^{\mathrm{OUT}} \quad \text{for} \quad i = 1\text{–}3 \tag{4}$$

$$\frac{\partial[\rho_{\mathrm{L}} \hat{U}_{\mathrm{L}} V_{\mathrm{L}}]}{\partial t} + \frac{\partial[\rho_{\mathrm{G}} \hat{U}_{\mathrm{G}}(V_{\mathrm{SEP}} - V_{\mathrm{L}})]}{\partial t} = G^{\mathrm{IN}} \hat{H}_{\mathrm{G}}^{\mathrm{IN}} - G^{\mathrm{OUT}} \hat{H}_{\mathrm{G}}^{\mathrm{OUT}} - L^{\mathrm{OUT}} \hat{H}_{\mathrm{L}}^{\mathrm{OUT}} + 2\pi(r_{\mathrm{SEP}} + x_{\mathrm{w_{SEP}}}) h_{\mathrm{wall}}(T_{\mathrm{w}} - T_{\mathrm{SEP}}) \tag{5}$$

where V_{L} is the volume of liquid retained in the column at a certain instant. The energy balance introduces a term that takes into account the heat flux supplied to the separation column by an external heating tape. h_{wall} is an effective heat transfer coefficient based on the temperature difference between the external wall and the inner temperature of the separation column. This can be set as an adjustable parameter in the dynamic model. The thermophysical properties are calculated at the temperature and pressure of the regeneration column.

Heat exchanger

The heat exchanger under consideration has a tube-in-tube configuration. High pressure carbon dioxide flows in the inner tube, while hot water flows countercurrently in the annular section. A dynamic model of such equipment was developed in a previous work.[11] Here, we present the main equations of the model. It is based on the following assumptions: negligible axial dispersion effects, fully developed turbulent flow in the tubes, and negligible heat losses to the environment. Given these assumptions, the unsteady energy balance for the gas flow in a differential volume of the inner tube is written as

$$\rho_{\mathrm{G}} \frac{\partial T_{\mathrm{G}}}{\partial t} + \frac{G}{\pi r_i^2} \frac{\partial T_{\mathrm{G}}}{\partial z} = \frac{2h_{\mathrm{G}}}{r_i C_{\mathrm{pG}}}(T_{\mathrm{wG}} - T_{\mathrm{G}}) \tag{6}$$

and that for the liquid in a differential volume of the annular space as

$$\rho_{\mathrm{L}} \frac{\partial T_{\mathrm{L}}}{\partial t} - \frac{L}{\pi[r_0^2 - (r_i + x_{\mathrm{wi}})^2]} \frac{\partial T_{\mathrm{L}}}{\partial z} = \frac{2(r_i + x_{\mathrm{wi}}) h_{\mathrm{L}}}{[r_0^2 - (r_i + x_{\mathrm{wi}})^2] C_{\mathrm{pL}}}(T_{\mathrm{wL}} - T_{\mathrm{L}}) \tag{7}$$

where r_{i} and r_{o} are the internal radius of the inner and outer tubes of the heat exchanger, respectively. T_{G} and T_{L} are the temperatures of carbon dioxide and liquid water flows. $T_{\mathrm{wG}} = T_{\mathrm{w}}|_{r=r_i}$ and $T_{\mathrm{wL}} = T_{\mathrm{w}}|_{r=r_i+x_{\mathrm{wi}}}$ stand for the gas and liquid temperatures at the inner tube walls. h_{G} and h_{L} are the gas-phase and liquid-phase heat-transfer coefficients, respectively.

The heat conduction flux through the inner tube wall is given by

$$\frac{\partial T_{\mathrm{w}}}{\partial_{\mathrm{t}}} = \frac{k_{\mathrm{w}}}{\rho_{\mathrm{w}} C_{\mathrm{pw}}} \left[\frac{\partial^2 T_{\mathrm{w}}}{\partial z^2} + \frac{1}{r} \frac{\partial}{\partial r} \left(r \frac{\partial T_{\mathrm{w}}}{\partial r} \right) \right] \tag{8}$$

where T_w stands for the inner wall temperature, and ρ_w and C_{pw} are the density and the specific heat of the wall material, respectively. The boundary conditions to the above set of differential equations are

$$T_G = (T_G)_{in} \quad \text{for} \quad z = 0 \tag{9}$$

$$T_L = (T_L)_{in} \quad \text{for} \quad z = H \tag{10}$$

$$\left(\frac{\partial T_w}{\partial z}\right)_{z=0,H} = 0 \qquad \text{for} \quad R_i \le r \le R_i + x_{wt} \tag{11}$$

and

$$k_w\left(\frac{\partial T_w}{\partial r}\right)_{r=R_i} = h_G(T_{wG} - T_G) \quad \text{for} \quad 0 \le z \le H \tag{12}$$

$$k_w\left(\frac{\partial T_w}{\partial r}\right)_{r=R_i+x_{wi}} = h_L(T_L - T_{wL}) \quad \text{for} \quad 0 \le z \le H \tag{13}$$

Make-up

In this unit, an additional quantity of carbon dioxide is fed to the SFE plant to compensate for the solvent losses that occur in the extraction and separation columns. It can be simply modeled by a set of material balances for each component of the mixture:

$$G^{IN}Y_i^{IN} + G^{make\text{-}up}Y_i^{make\text{-}up} = G^{OUT}Y_i^{OUT} \quad \text{for } i = 1-3 \tag{14}$$

where G^{IN} represents the mass flow of gas phase entering the make-up unit. The gas phase make-up flow, $G^{make\text{-}up}$, consists of carbon dioxide only.

The individual dynamic models of the extraction column, the solvent feed heat exchanger, the regeneration column, and the solvent make-up were all combined to create the dynamic simulation model of the SFE plant. The gas phase output stream from the heat exchanger is made equal to the input solvent stream of the extraction column. The extract phase output conditions from the packed column are used to compute the input gas phase conditions to the separation column. Finally, the solvent stream exiting the separation column is further mixed with the make-up stream of pure carbon dioxide and the resulting stream is forward to the inlet of the heat exchanger.

Numerical solution

The complete system of partial differential and algebraic equations of the dynamic model is solved by uncoupling the spatial and time discretisation; the original partial differential equations of each SFE model unit are converted into a system of ordinary differential and algebraic equations (DAEs) with respect to time. The DAE system thus obtained is integrated in time using the commercial process simulation software package gPROMS.[12]

Validation of SFE Plant Model

The dynamic model of the SFE plant process can be very useful to study the dynamic behavior of a SFE process. If it can represent the real performance of the process to a reasonable degree of accuracy, it can be further employed for control and process optimization purposes. SFE processes are very sensitive to changes in main operating variables, such as the pressure and temperature of extraction and the solvent flow rate. When a perturbation on one of these variables occurs, the extract and raffinate compositions may change abruptly, which in turn may affect the efficiency of the regeneration step (that is, the separation column); ultimately, the regenerated solvent stream can re-enter the extraction column, partially saturated in solutes, thus affecting the mass transfer efficiency of the extraction. The process simulator can be used to test the response of the SFE plant to induced perturbations in the main operating variables.

The dynamic model of the SFE process was validated by comparing the results predicted by the process simulator with experimental data obtained in a pilot-scale SFE apparatus. The tests were performed using as a case study—the fractionation of the binary mixture squalene/methyl oleate by supercritical carbon dioxide. Experimental data on the phase equilibrium and mass transfer of this system was already measured and presented elsewhere.[5,10]

The main characteristics of each unit in the pilot-scale SFE plant are shown in Table 1. A data acquisition system connected to the SFE pilot-plant allows the online recording of the pressure, temperature, and mass flow rates of the two fluid phases within the apparatus. For each extraction run, samples of the raffinate and extract streams from the extraction column, and of the liquid phase collected at the bottom of the separation column were taken at constant time intervals, and their composition analyzed for the squalene content by refractive index. This analytical method was previously checked against gas chromatography and was found to be a useful and rapid tool for data analysis. A detailed description of an extraction experiment can be found elsewhere.[10]

A specific number of experimental runs were performed in this work, where disturbances in specific process variables were generated and the response of the whole SFE process to those perturbations analyzed. The process variables were

Table 1. Main Characteristics of SFE Plant for Process Simulation

Extraction column	
Packing type	Sulzer EX
Total packed bed height, m	2
Internal diameter, mm	24
Surface area of packing, m^2/m^3	1710
Void fraction of packing	0.86
Crimp height (h), mm	1.6
Channel base ($2b$), mm	4
Side of corrugation (s), mm	2.9
Channel flow angle from the horizontal (θ), degrees	45
Separation column	
Height, m	1
Internal diameter, mm	24
Wall thickness, mm	7
Heat exchanger	
Inner tube—Stainless steel AISI 316	
Outer diameter, mm	6.35
Wall thickness, mm	1.8
Outer tube—Copper	
Outer diameter, mm	50
Total length, m	0.8

Table 2. Experimental SFE Runs

Run no.	Description (Feed flowrate, 0.3 kg/h)
1	Feed composition, 48 wt % squalene Gas flowrate, 7.2 kg/h T_{EC}, 323 K P_{SC}, 6.5 MPa T_{SC}, 333 K P_{EC}: at start, 15.0 MPa; at 70 min, 12.0 MPa
2	Feed composition, 42 wt % squalene Gas flowrate, 4.8 kg/h P_{EC}, 15.0 MPa P_{SC}, 6.5 MPa T_{SC}, 333 K T_{EC} (in average) at start, 323 K; at 65 min, set point of heating tapes controllers at 293 K; at 147 min, set point of heating tapes controllers at 313 K
3	Feed composition, 38 wt % squalene P_{EC}, 15.0 MPa T_{EC}, 323 K P_{SC}, 6.5 MPa T_{SC}, 333 K Gas flowrate: at start, 4.8 kg/h; at 95 min of run, 9.6 kg/h
4	P_{EC}, 15.0 MPa T_{EC}, 323 K P_{SC}, 6.5 MPa T_{SC}, 343 K Gas flowrate, 4.8 kg/h Feed composition: at start, 40 wt % squalene; at 75 min of run, 70 wt % squalene
5	Feed composition, 40 wt % squalene Gas flowrate, 4.8 kg/h P_{EC}, 15.0 MPa T_{EC}, 323 K T_{SC}, 333 K P_{SC}: at start, 7.0 MPa; at 105 min, 10.0 MPa
6	Feed composition, 45 wt % squalene P_{EC}, 15.0 MPa T_{EC}, 323 K P_{SC}, 6.0 MPa T_{SC}, 333 K Gas flowrate: 8.4 kg/h; At 85 min: gas pump shut down

selected according with their importance to the effectiveness of a SFE process, namely, the pressure and temperature conditions of the extraction column and of the separation/regeneration column, the solvent flow rate, and the composition of the liquid mixture fed to the extraction column. The flowrate of the liquid feed was kept constant throughout the whole set of experiments due to a limited pump capacity. An additional run was carried out where a "accidental" shutdown was induced to the apparatus by switching off the solvent pump at a certain extraction time.

A description of the experimental runs with the respective composition and flow rate of the feed, the solvent flow rate, the pressure, and temperature conditions of the extraction and separation columns is listed in Table 2.

Figures 4 and 5 show the responses of the experimental and predicted extract and raffinate compositions to an induced perturbation in the pressure and temperature of the extraction column, respectively. The compositions are expressed in mass fraction of solute i in a solvent free basis.

The predicted extract composition shows excellent agreement with the experimental values, while the raffinate compositions shows a deviation in some sections of the extraction runs. Moreover, in the first period of extraction (up to ~500 s of extraction), the predicted extract composition shows a deviation to the experimentally observed. This deviation is probably due to the fact that the dynamic model of the extraction column has a singularity as $h_L \rightarrow 0$. To circumvent this problem, it is assumed that a minimum amount of liquid phase with a predefined composition is already present in the packed bed at start-up so that the model can converge in the first instants of extraction. Therefore, the predicted composition of the extract at the first period of extraction corresponds to a condition that does not reflect the real behavior of the extraction column. The observed deviation of the predicted raffinate composition has been reported before[4] and may be attributed to a wrong adjustment of the mass transfer equations to this system at some operating conditions.

The induced perturbation in the pressure of the extraction column had a much larger effect on the fractionation of the binary mixture methyl oleate/squalene than in the temperature of extraction. Reducing the pressure from 15.0 to 12.0 MPa resulted in an increase of the selectivity of carbon dioxide (higher purity of the extract stream on methyl oleate)

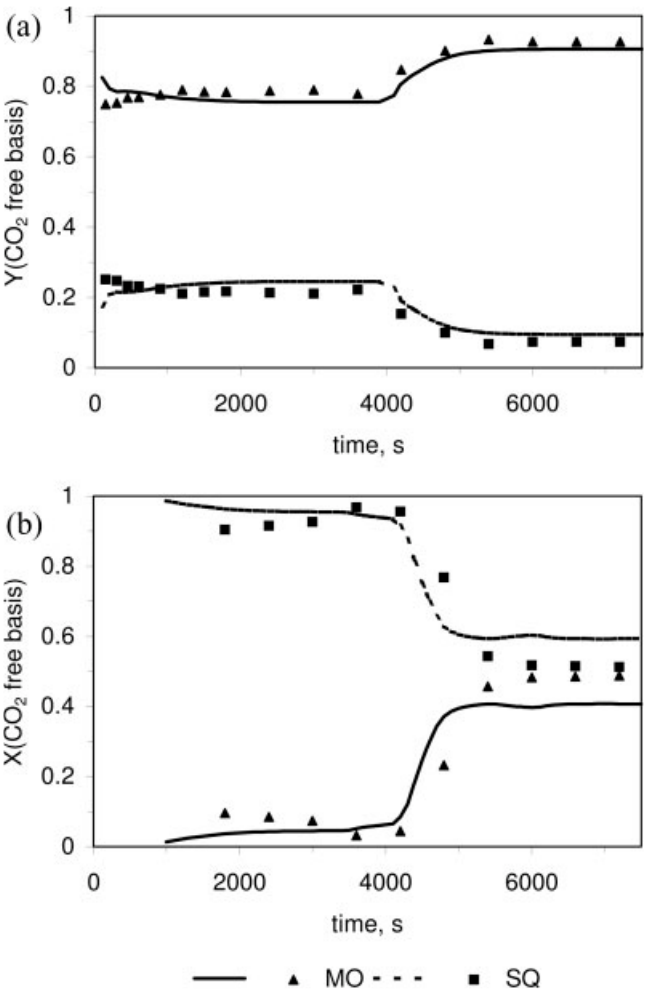

Figure 4. Induced perturbation in the extraction pressure.

Mass fraction of methyl oleate (MO) and squalene (SQ), in a solvent free basis, of the extract (a) and raffinate (b) streams. Symbols: experimental data; lines: predicted data.

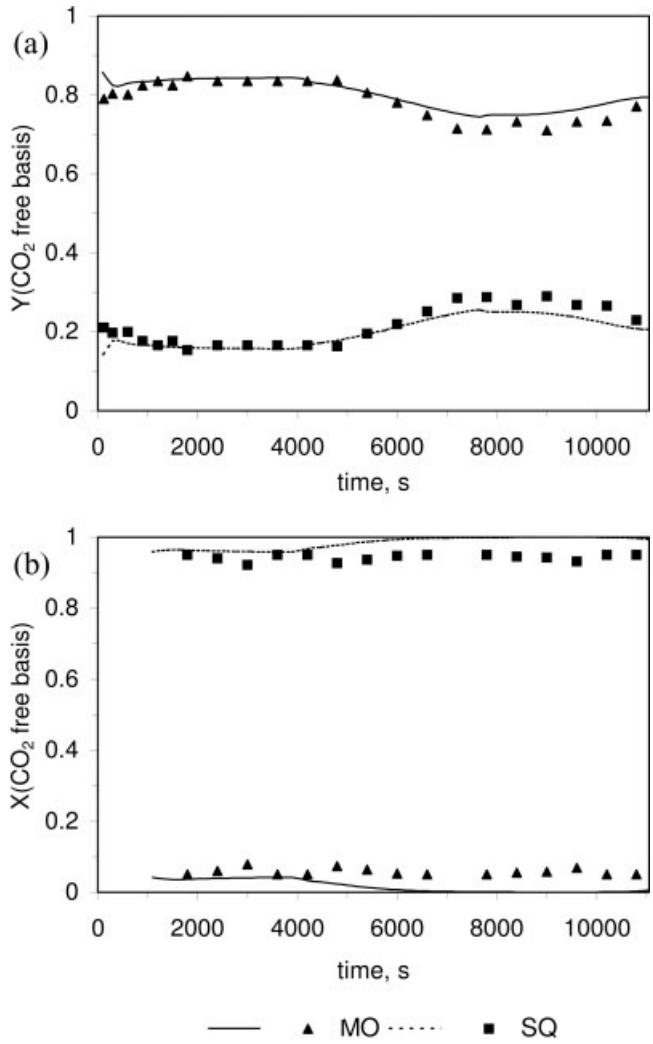

Figure 5. Induced perturbation in the extraction temperature.

Mass fraction of methyl oleate (MO) and squalene (SQ), in a solvent free basis, of the extract (a) and raffinate (b) streams. Symbols: experimental data; lines: predicted data.

but with the payback of obtaining a much load throughput. That is, the amount of solutes dissolved by the solvent decreased with the consequence of the raffinate stream had a composition almost similar to the feed composition. The change in the temperature of extraction did not result in a substantial response of the process; this may be attributed to the fact that the perturbation was created by simply changing the set-point of the heating tapes surrounding the column wall from 323 to 293 K. Yet, this resulted in a change of the internal temperature of the packed bed by less than 10° in more than one and half hours of experiment.

Figure 6 shows the response of the experimental and predicted extract and raffinate compositions to an induced perturbation in the solvent flow rate. Additionally, it also shows the effect of this change in the liquid phase collected at the bottom of the separation column (X'_{OUT}; Figure 3). Again, the predicted extract compositions show a very good fit to the experimental data, while the simulated raffinate composition does not match the observed after the step change in the solvent flow rate at about 95 min of extraction. This deviation is probably due a limitation of the hydrodynamic and mass transfer model used by the dynamic model. Further work will be done to determine how buoyancy and axial dispersion effects influence the fluid dynamics in the packed bed. The predicted liquid phase composition at the bottom of the separation column shows an excellent agreement with the experimental values. The same trend was observed for the response of the experimental and simulated stream compositions to an induced perturbation in the liquid feed composition (run no. 4, Table 2). The dynamic simulator was able to

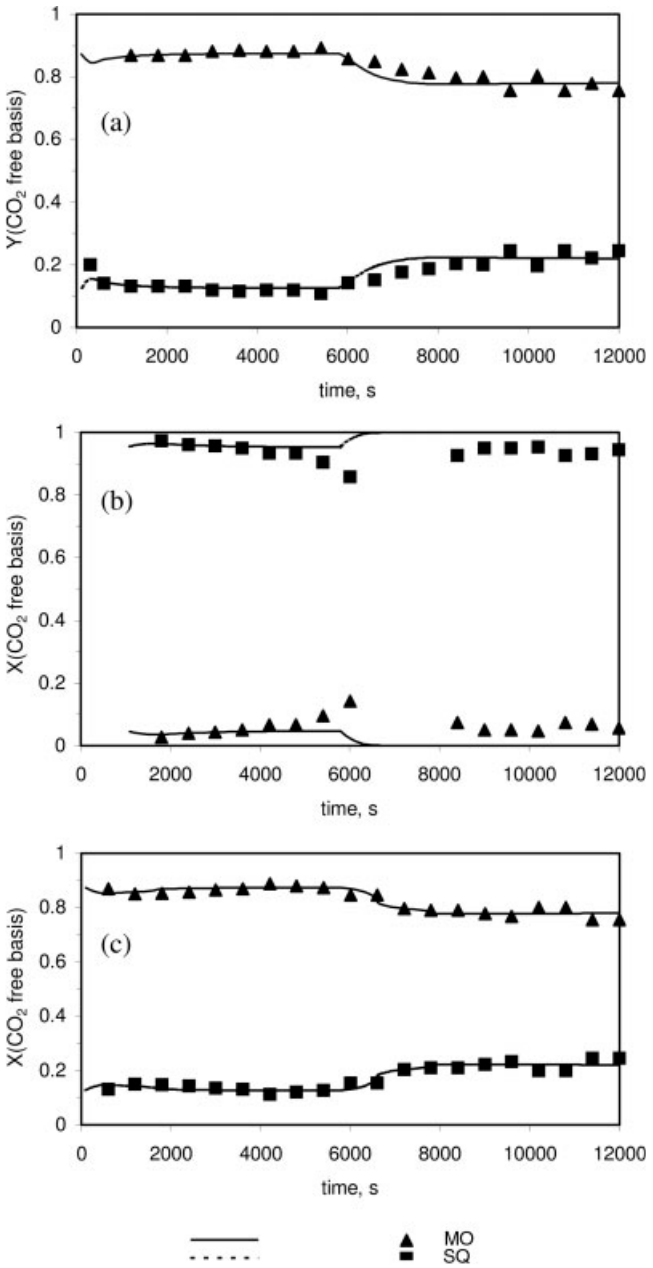

Figure 6. Induced perturbation in the solvent flow rate.

Mass fraction of methyl oleate (MO) and squalene (SQ), in a solvent free basis, of the extract (a), raffinate (b), and liquid phase at bottom of separation column (c). Symbols: experimental data; lines: predicted data.

predict correctly the response of the extract composition and of the liquid phase collected at the bottom of the separation column to a sudden enrichment in squalene of the feed stream to the extraction column; yet, the predicted raffinate composition showed a small deviation in the experimental data.

Figure 7 presents the effect of a perturbation in the separation column pressure on the respective outlet phase compositions and raffinate composition of the extraction column. Although the model was able to predict a proper response of the stream compositions to the change in the separation pressure, it is clear that the simulated data deviates substantially from the experimental data in some moments of the run. One reason may be the method used to increase the pressure of the separation column. Technically, this was carried out by manually closing a back separator valve installed at the gas phase pipe section exiting the separation column. This process not only increased the pressure of the separation column but also created a perturbation in other variables of the process, such as, the temperature of the column and the gas flow rate of the solvent. It is possible that these perturbations were not correctly fitted to the dynamic model of the SFE plant. Moreover, the separation column was modeled as a theoretical stage in which thermodynamic equilibrium was assumed to occur inside the vessel between the gas phase and the precipitated liquid phase. For the most part of the runs, the model predicted correctly a 100% regeneration of the solvent and a complete recovery of the precipitated solutes at the bottom of the column, as it was experimentally observed. Yet, the response of the predicted outlet gas and liquid phase compositions to a perturbation in the separation pressure showed a clear deviation from the experimental data. This deviation can be attributed to the thermodynamic model employed for the calculations of the outlet phase compositions. The thermodynamic correlation used for the extraction column conditions (and derived from previously collected experimental data for the ternary system methyl oleate + squalene + carbon dioxide) was further extended to cover the operating conditions of the separation column. It is fairly possible that the extended thermodynamic correlation was not valid for some of the conditions of temperature and pressure of the separation column we used in the SFE tests. A better fitting may be obtained if additional experiments are made to collect thermodynamic data at those operating conditions.

Although the model showed some deviations from the experimental data, it can be nevertheless useful for control purposes of similar SFE processes. Run 6 was initially carried out with the purpose of induce a perturbation in the temperature of the extraction column. Yet, after ca. 80 min of extraction, and unexpectedly, carbon dioxide run out in the respective gas cylinder. As a consequence, gas flow rate decreased abruptly as well as the extraction pressure. This incidental shutdown test turned to be perfect to assess the ability of our dynamic model to predict the response of the SFE plant to a sudden shutdown situation and compared it against the experimental data. Figure 8 shows the changes in the solvent flow rate and extraction pressure and the responses of the predicted and experimental extract and raffinate compositions. It also plotted the loading of carbon dioxide (in grams of solubilized oil per kilograms of carbon dioxide) in the extract phase. The response of the raffinate composition is well predicted by the model; moreover, it predicts small fluctuations

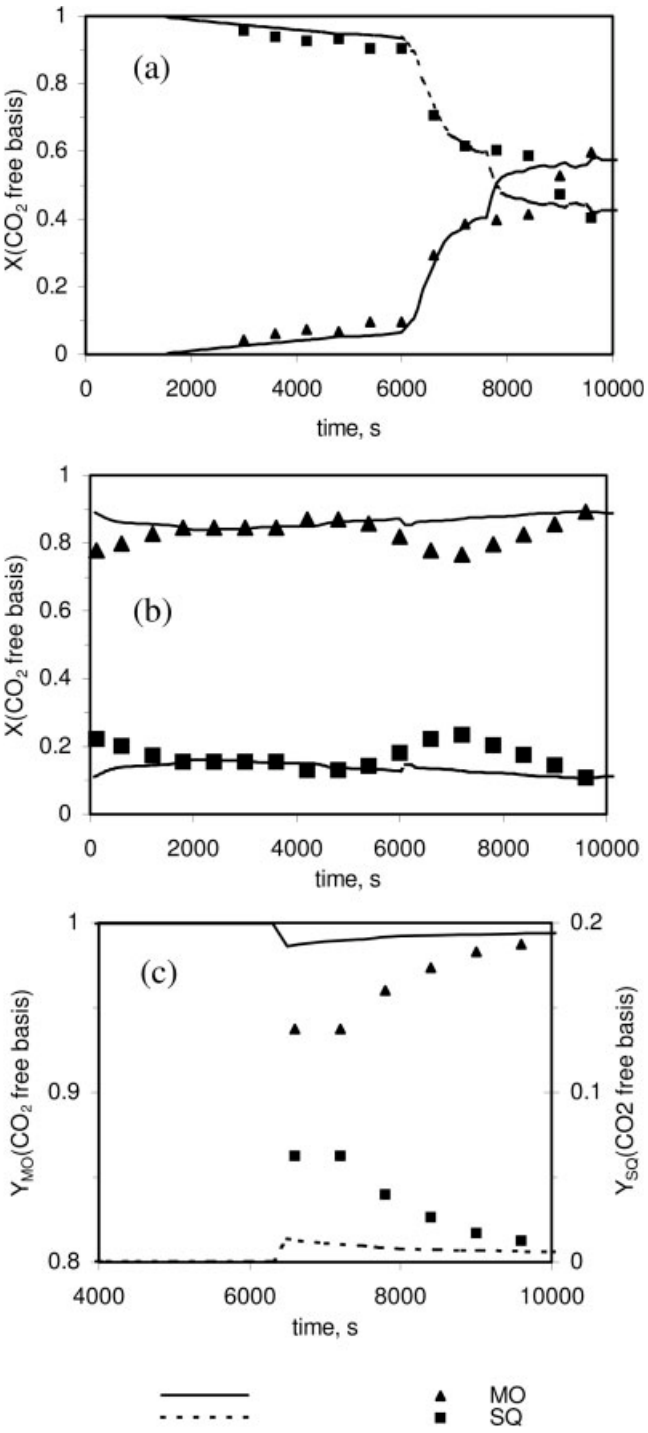

Figure 7. Induced perturbation in the separation pressure.

Mass fraction of methyl oleate (MO) and squalene (SQ), in a solvent free basis, of the raffinate phase of extraction column (a) and the outlet phases of separation column (b and c). Symbols: experimental data; lines: predicted data.

in the composition that were not possible to detect experimentally. The shutdown of the gas flow rate—although not total—had as a consequence the decrease in the loading of carbon dioxide exiting the extraction column. The model was able to predict this behavior qualitatively, if not quantitatively.

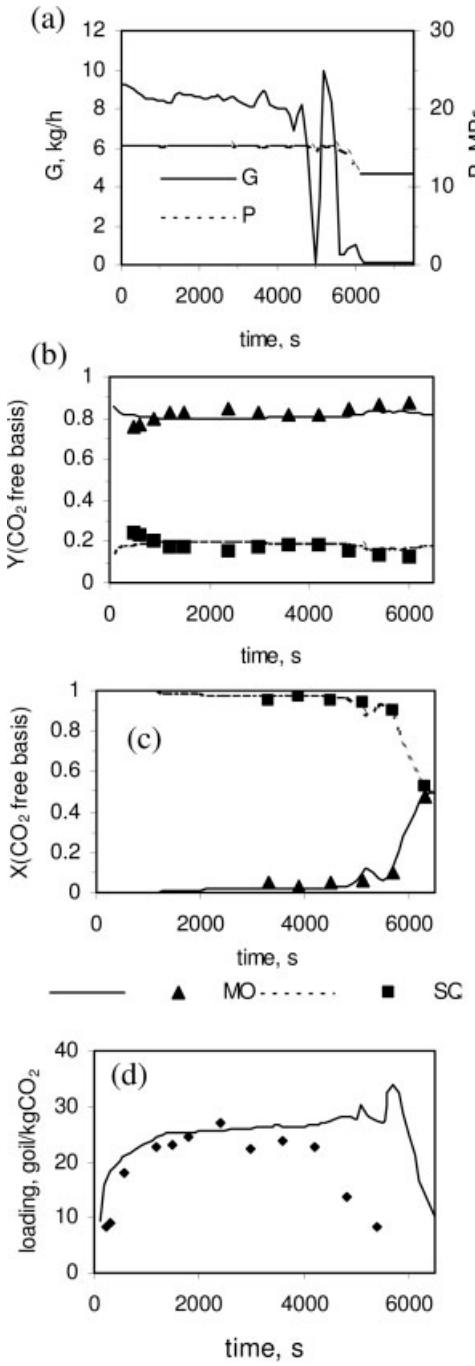

Figure 8. Solvent flowrate and extraction pressure changes in run 6 (a); mass fraction of methyl oleate (MO) and squalene (SQ), in a solvent free basis, of the extract (b) and raffinate (c) streams; loading of extract phase (d).

Symbols: experimental data; lines: predicted data.

Application of EC Model to SFE Case Studies

The dynamic model of the high pressure packed extraction column was applied to several SFE case studies to assess its general application to SFE processes. The criteria used to select the case studies were the existence of reliable experimental data available in the literature and a potential industrial application of the process. The selected case studies were the deacidification of VOO by SC CO_2,[6] the fractionation of OODD by SC CO_2,[7] the fractionation of SLO by SC CO_2,[8] and R134a.[9]

The input variables of the simulation model for each system were the flow rates and compositions of the solvent and liquid feed inlet streams, and the initial values of the pressure and temperature of extraction. The experimental thermodynamic equilibrium data, the mass transfer, and hydrodynamic data for each system were collected from the literature.[6–9,13,14] The physical properties of the gas and liquid phases were taken from experimental data if available or, otherwise, calculated by common estimation methods.[15] Table 3 presents the whole set of operating conditions tested in this work for all the case studies under analysis.

For each case study, a preliminary evaluation of the accuracy of the experimental data available was made. From the whole set of data, a sensible number of extraction runs were selected and each one replied by the dynamic model. For each simulated experiment, the composition profiles of the gas and liquid phases were determined as a function of extraction time and axial position in the packed column. The comparison between the experimental and predicted results, for each extraction run, was made by comparing the compositions of the extract and raffinate streams at *steady state* conditions. This procedure was taken because in most part of the selected case studies there was no information available on the nonstationary period of extraction. In addition, most part of the reference works presented the composition of the outlet streams from the extraction column in terms of solute mass fraction in a solvent free basis. Accordingly, we opted to use this variable in our comparisons.

Table 4 gives the average relative deviation (ARD) of the predicted compositions of the extract and raffinate phases at steady state conditions to the experimental data. The ARD of the extract phase composition is lower than 10% in overall, which shows good agreement between experimental and predicted data. A higher overall ARD was obtained for the raffinate phase compositions. It is possible that this higher value may be attributed to a higher error of the corresponding experimental data; in average, the raffinate phase compositions (in a CO_2-free basis) were of a much lower magnitude than the corresponding extract phase compositions. It should be pointed out that the hydrodynamic and mass transfer equations used by the dynamic model were the same as the ones suggested in the reference works for each case study. It is likely that the effectiveness of the simulation model for a particular SFE system could be further improved by considering other correlations.

Although the comparison of the predicted results against the experimental data was only made for steady state conditions, nevertheless, the dynamic model can be of help by providing a reasonable indication on the composition profiles of the gas and liquid phases with the axial position in the packed column and the extraction time. Figures 9 and 10 show the calculated steady state composition profile (in a solvent-free basis) of the gas and liquid phases with the packing height, for the case of the deacidification of VOO by SC CO_2. To simplify calculations, the multicomponent system

Table 3. Range of Operating Parameters According to Process System Under Analysis

System	d_i, mm	z, m	Column Packing	P, bar	T, °C	Phase	Flow Rate, Kg h^{-1}	Re Number	Loading g_{oil}/kg_{SCF}	Ref.
VOO/CO_2*	24	1	Sulzer CY	128–208	40, 50	Oil phase	0.1–0.3	$2 \times 10^2 - 6 \times 10^2$	1–4	6
						Solvent phase	1–7	75–500		
	17.5	6	Sulzer EX	210–310	80	Oil phase	0.1–0.2	$3 \times 10^2 - 8 \times 10^2$	2–9	13
						Solvent phase	3–6	200–450		
OODD/CO_2†	24	1	Sulzer CY	128, 148	40, 50	Oil phase	0.2	2×10^2	5	–
						Solvent phase	2–6	100–200		
	17.5	6	Sulzer EX	200, 230	77, 97	Oil phase	0.13	–	2–9	7
						Solvent phase	3–4			
SLO/CO_2‡	56	2.5	Raschig rings	200, 250	40, 60	Oil phase	0.3–1.2	0.1–0.45	10–30	8
						Solvent phase	10–30	200–400		
	205	1.9	Fenski spirals	250, 300	60	Oil phase	10–20	0.5–1.2	10–25	8
						Solvent phase	300–400	600–800		
SLO/R134a§	56	2.5	Raschig rings	60	60–80	Oil phase	0.2–0.5	$4 \times 10^2 - 12 \times 10^2$	2–8	9
						Solvent phase	17–22	200–300		

*Modeled as the pseudoternary system oleic acid + triolein + carbon dioxide.
†Modeled as the pseudoquaternary system oleic acid + methyl oleate + squalene + carbon dioxide.
‡Modeled as the pseudoternary system squalene + triglycerides + carbon dioxide.
§Modeled as the pseudoternary system squalene + triglycerides + R134a.

was modeled as the pseudoternary system free fatty acids (FFA) + triglycerides (TRIG) + carbon dioxide. For comparison, it also plotted the experimental steady state compositions of the extract and raffinate phases. Figure 9 presents experimental data obtained with a lab-scale column of 1 m packing height (Sulzer CY packing) and 2.4 cm of internal diameter[6]; Figure 10 shows experimental data obtained with a pilot-scale fractionation column with 6 m packing height (Sulzer EX packing) and 17.5 mm of internal diameter.[13] The correspondent extraction conditions are indicated in the respective legends. Both figures illustrate the high selectivity of carbon dioxide towards the free fatty acids as observed experimentally. A reduction in the acidity of olive oil to less than 2 wt % in the raffinate phase was achieved in the pilot-scale packed column with a simultaneous relatively rich extract phase on free fatty acids.

The approach to steady state conditions can be visualized in Figure 11 for the same system, where the solvent-free mass fraction of free fatty acids in the raffinate and extract phases are plotted as a function of the extraction time. Predicted data was calculated for the pilot-scale fractionation column case. Clearly, less than 1 h of extraction is needed to achieve steady state conditions in the extraction column. The extract phase acidity shows a peak at the first moments of extraction, which can be attributed to the startup conditions of the simulation model. This requires a minimum amount of liquid phase in the extraction column to be present at the beginning of the simulation run.

Table 4. Average Relative Deviation (ARD) of Compositions of Raffinate and Extract Streams (in a Solvent Free Basis) as Predicted by the Dynamic Model

	ARD (%)	
System	Y'_{out}	X'_{out}
VOO/CO_2	8.3	28.1
OODD/CO_2	12	15
SLO/CO_2	4.0	36.5
SLO/R134a	15.9	26.5
Overall	*9.2*	*26.6*

Figure 12 shows the calculated and experimental composition profiles (in a solvent-free basis) of the gas and liquid phases for the fish oil/CO_2 system. The experimental extraction data were obtained in a pilot scale packed column of 56 mm of internal diameter and 2.5 m of packing height, with 8.5 mm glass Raschig rings.[8] The raw SLO used in the experimental run contained 50% by weight squalene and the rest made of TRIG. The simulation run correctly predicted the extract and raffinate phase compositions at steady state conditions.

The efficacy of the simulation model to high pressure systems with other near-critical solvents than carbon dioxide was assessed by applying the model to the fractionation of SLO by the alternative refrigerant R134a (1,1,1,2-tetrafluoroethane). Experimental data on the transient period of the extraction process was recorded for this system in terms of

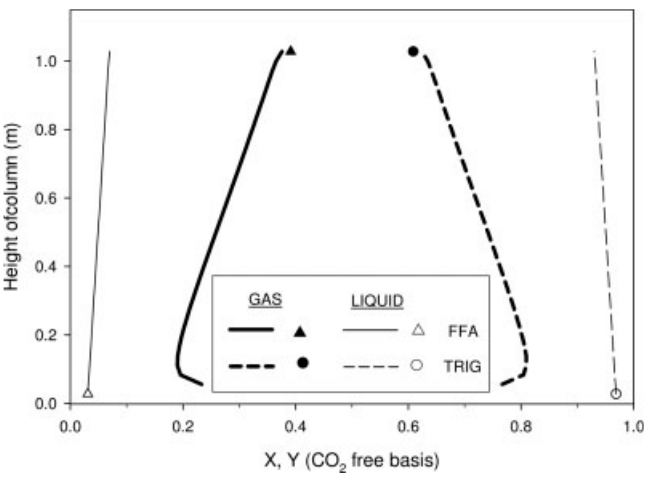

Figure 9. Composition profile of the gas and liquid phases with packing height at steady state for the VOO/CO_2 system.

Operating conditions: 17.8 MPa/323 K, G_{in}/L_{in} = 45. Symbols refer to experimental data[6] and lines to modelling results.

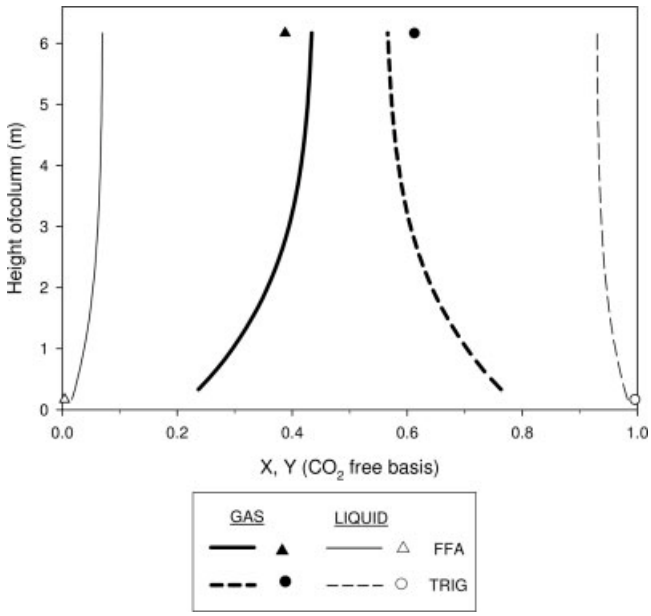

Figure 10. Composition profile of the gas and liquid phases with packing height at steady state for the VOO/CO_2 system.

Operating conditions: 26.0 MPa/353 K, G_{in}/L_{in} = 30. Symbols refer to experimental data[13] and lines to modelling results.

the mass fraction compositions of raffinate and extract streams.[9] The extract stream was collected in two separate fractions by using a sequence of two gravimetric separation vessels, named as SV1 and SV2. Figure 13 shows the predicted and experimental squalene composition, in a solvent free basis, of the extract phase collected at the bottom of the

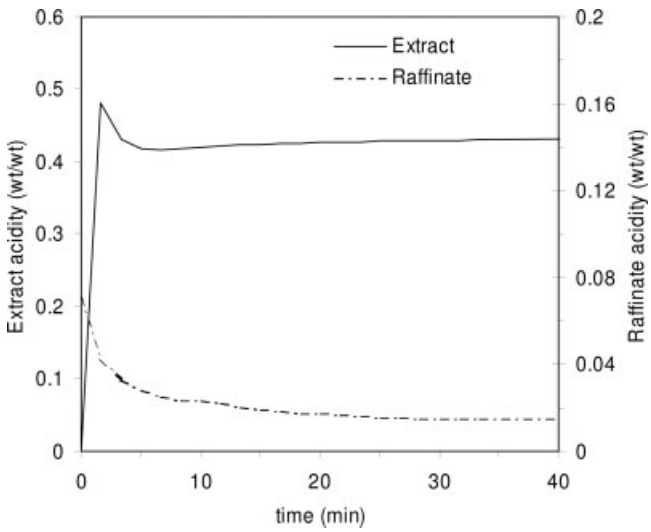

Figure 11. Free fatty acids weight composition (in a solvent free basis) in the raffinate and extract phases as a function of extraction time.

Operating conditions: 26.0 MPa/353 K, G_{in}/L_{in} = 30.

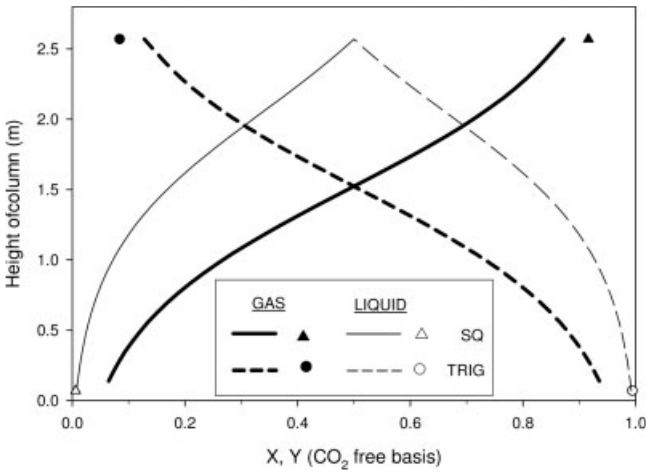

Figure 12. Composition profile of the gas and liquid phases with packing height at steady state, for the SLO/CO_2 system.

Operating conditions: 25.0 MPa/333 K, G_{in}/L_{in} = 35. Symbols refer to experimental data[8] and lines to modelling results.

two separators as a function of the extraction time. Both separators were held at the same pressure (0.6–0.7 MPa) but at different temperatures of 293 and 313 K, respectively. The model predicts the correct compositions of the extracts collected in the two vessels for steady state conditions; clearly, there is a visible discrepancy between the experimental and simulated data in the unsteady state period. The SFE pilot plant used for the experimental extraction runs with the SLO/R134a system did not allow the online recording of the main operating variables, i.e., the pressure and temperature of the extraction column and the two separation vessels, as well as the flowrates of gas and liquid phases with time. It is possible that significant fluctuations on these variables at the beginning of the extraction run may cause the above difference.

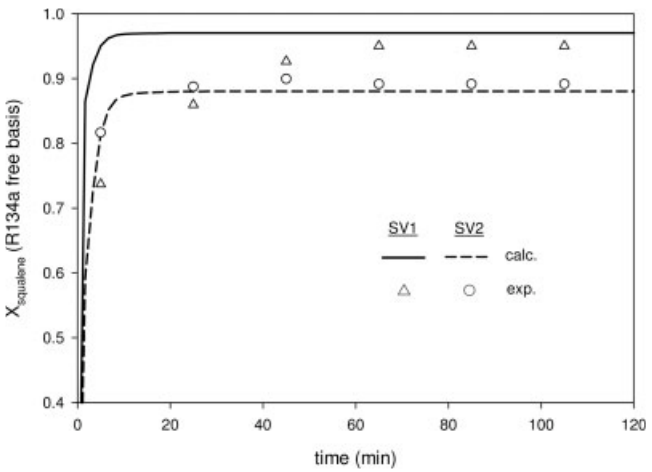

Figure 13. Composition profile of the liquid phases collected at separator vessels for the SLO/R134a system.[9]

Operating conditions: 6.0 MPa/353 K, G_{in}/L_{in} = 50.

Conclusions

A dynamic model of a SFE plant was developed by incorporating specific models for the main plant units: the extraction packed column, the regeneration column, the high pressure solvent heat exchanger, and the solvent make-up. The simulation model was applied to the fractionation of the binary mixture squalene/methyl oleate by supercritical carbon dioxide. A set of experiments was performed in a pilot-scale SFE plant where disturbances in specific process variables were generated and the response of the whole SFE process to those perturbations recorded. The experimental data was compared to the predicted by the simulation model. A close agreement was verified to exist which validates the current model as a valid computational tool for design and optimisation of SFE processes. Yet, some deviations between the experimental and predicted responses of the fluid compositions were observed; they should be attributed to the actual mass transfer and hydrodynamic model of the extraction column and the thermodynamic equilibrium model of the separation column. Future work will be done to improve the efficiency of the SFE dynamic model.

To further test the current dynamic model, the simulation unit of the high pressure packed column was validated by comparing the model's predictions with experimental data available in the literature for several SFE processes. A relatively good agreement was found to exist between experimental and calculated results for all the extraction runs tested in this work. Unfortunately, only steady state results were possible to be validated for most part of cases, since no information was available in the literature regarding the respective transient period of extraction. Nevertheless, we believe the model could be applied for such conditions once reliable technical data is provided for a specific SFE test.

The model was not able to predict correctly the raffinate phase concentrations for some cases; this can be attributed either to the dynamic model effectiveness or to the quality of the experimental data collected from the literature. The relative uncertainness of the collected data introduces a nonnegligible factor on the ARD obtained by the model that cannot be ascertained. Moreover, in some cases, the operating conditions for a specific extraction run were not completely explicit in the reference work, which caused an obvious problem to run the simulation model. Nevertheless, it is believed that the main factor for the relative uncertainty of the dynamic model is due to the use of a wrong or incorrect model for the thermodynamic equilibrium and/or mass transfer in the simulation tool. In some cases, the available experimental thermodynamic data was limited to a specific range of operating conditions of pressure, temperature, and composition that do not entirely crossover the range of operating conditions studied for the respective extraction experiments. Since the selectivity of a supercritical solvent for a specific mixture is highly dependent on the composition, the lack or partial knowledge of this information hinders the efficiency of the dynamic model. The mass transfer and hydrodynamics equations provided to the dynamic model were, as stated before, the ones suggested in the reference works. It is quite possible that alternative correlations could improve the effectiveness of the dynamic model.

In summary, the results obtained in this work show that the dynamic simulator of the SFE plant is reliable in its use to general SFE processes of liquid mixtures and can be of great help to the design and optimization of these processes.

Acknowledgments

Financial support by Fundação para a Ciência e Tecnologia, under project grant number POCTI/EQU/61550/2004, and grants SFRH/BD/19243/2004 and SFRH/BPD/14635/2003 are acknowledged.

Notation

A = cross section area of extraction column, m^2
G = gas mass flowrate, kg/s
$\hat{H}$ = enthalpy, J/kg
h_L = liquid holdup
J = interphase mass transfer flowrate
k = thermal conductivity, W/m K
L = liquid mass flow, kg/s
P = pressure, Mpa
R = ideal gas constant, 8.31451 J/(K mol)
r = radius, m
t = time, s
T = temperature, K
$\hat{U}$ = internal energy, J/kg
V = volume, m^3
X = liquid phase mass fraction composition
X' = liquid phase composition in a solvent free basis
Y = gas phase mass fraction composition
Y' = gas phase composition in a solvent free basis
z = column axial coordinate, m

Greek letters

ε = packing void fraction
ρ = density, kg/m^3

Subscripts

i = component
in = initial
G = gas
L = liquid
SEP = separation column
OUT = exit stream from column
w = wall conditions

Literature Cited

1. Cygnarowicz M, Seider W. Design and control of a process to extract β-carotene with SC CO_2. *Biotech Prog*. 1990;6:82–91.
2. Hytoft G, Gani R. Simulation tools for design and analysis of SCE processes. Presented at AICHE Annual Meeting, St Louis, MI, November, 1993. Paper Nr 9c, 251.
3. Ramchandran B, Riggs JB, Heichelheim HR, Seibert AF, Fair JR. Dynamic simulation of a supercritical fluid extraction process. *Ind Eng Chem Res*. 1992;31:281–290.
4. Ruivo R, Paiva A, Mota JPB, Simões P. Dynamic model of a countercurrent packed column operating at high pressure conditions. *J Supercrit Fluids*. 2004;32:183–192.
5. Ruivo R, Cebola MJ, Simões PC, Nunes da Ponte M. Fractionation of edible oil model mixtures by supercritical carbon dioxide in a packed column, Part 2: A mass transfer study. *Ind Eng Chem Res*. 2002;41:2305–2315.
6. Carmelo PJ, Simões PC, Nunes da Ponte M. Modelling of mass transfer in supercritical countercurrent extraction column: Application to olive oils. *Chem Biochem Eng Q*. 1994;8:5–9.

7. Buss D, Brunner G. Countercurrent extraction with supercritical carbon dioxide: Behavior of a complex natural mixture. In: *Forschungszentrum Karlsruhe—Technik Und Umwelt, Wissenschaftliche Berichte* (Dahmen N, Dinjus E. Editors), Karlsruhe, 1999: 197–200. In HP Chemical Engineering Meeting, Karlsruhe, Germany, 1999.
8. Catchpole OJ, von Kamp J-C, Grey JB. Extraction of squalene from shark liver oil in a packed column using supercritical carbon dioxide. *Ind Eng Chem Res*. 1997;36:4318–4324.
9. Simões PC, Catchpole OJ. Fractionation of lipid mixtures by subcritical R134a in a packed column. *Ind Eng Chem Res*. 2002;41:267–276.
10. Ruivo R, Cebola MJ, Simões PC, Nunes da Ponte M. Fractionation of edible oil model mixtures by supercritical carbon dioxide in a packed column, Part 1: Experimental results. *Ind Eng Chem Res*. 2001;40:1706–1711.
11. Simões PC, Fernandes J, Mota JP. Dynamic model of a supercritical carbon dioxide heat exchanger. *J Supercrit Fluids*. 2005;35:167–173.
12. Process Systems Enterprise. *gPROMS v2.0. Introductory User Guide*. London: Process Systems, 2001.
13. Simões PC, Brunner G. Multicomponent Phase Equilibria of an extra-virgin olive oil in supercritical carbon dioxide. *J Supercrit Fluids*. 1996;9:75–81.
14. Catchpole OJ, von Kamp J-C. Phase equilibrium for the extraction of squalene from shark liver oil. *Ind Eng Chem Res*. 1997;36:3762–3768.
15. Reid RC, Prausnitz JM, Poling BL. *The Properties of Gases and Liquids, 4th ed*. New York: McGraw-Hill, 1987.

Manuscript received Mar. 16, 2006, revision received Oct. 3, 2006, and final revision received Jan. 3, 2007.